

# Determination of Vibrational Displacement Measurement Error Based on the Blurring Analysis of a Round Mark Image

Alexey Grigorev<sup>1</sup>, Alexey Lysenko<sup>2</sup>, Igor Kochegarov<sup>3</sup>, Vladimir Roganov<sup>4</sup>, Jurijs Lavendels<sup>5\*</sup>

<sup>1-3</sup>*Penza State University, Penza, Russia*

<sup>4</sup>*Penza State Technological University, Penza, Russia*

<sup>4</sup>*Penza State University of Architecture and Construction, Penza, Russia*

<sup>5</sup>*Riga Technical University, Riga, Latvia*

**Abstract** – The relevance and nature of a new technology for measurement of vibrational displacement of a material point through normal toward the object plane are stated in the article. This technology provides registration and processing of images of a round mark or a matrix of round marks, which are applied to the surface of a control object. A measuring signal here is the module of radius increment of the round mark image at vibrational blurring of this image. The method for calculation of the given error of measurements, as a function of a number of pixels of the round mark image, has been developed and proven in the present research. The results of pilot studies are given. Linearity of transformation of the measured size into a measuring signal has been proven. The conditions of a technical compromise between the field of view area of a recording device during distribution measurement of vibrational displacements along the surface of a control object, and the accuracy of this measurement are determined. The results are illustrated with numerical examples of calculations of the given error of measurements in the set field of view and the one at the given maximum set error of measurements.

**Keywords** – Accuracy, blurring, displacement, error, image, raster unit, measurement, vibration.

## I. INTRODUCTION

Onboard radio-electronic equipment of rocket-space and transport vehicles is subjected to vibrations in the process of operation, including high-frequency ones. The frequency range of vibration effects varies from units of hertz to several tens of kilohertz. Tests of experimental and layout prototypes of such equipment on vibration stands allow revealing problem design sites, and developing a vibration protection strategy. The vibration measurement of the onboard radio-electronic equipment during operation makes it possible to predict vibration resistance of the structure, and to detect defects in the equipment in their latent phase, i.e., at the stage of their origin and development. Let us consider setting the problem of refinement of vibration parameters and one of the solution algorithms.

## II. A REVIEW OF EXISTING APPROACHES

External vibration effects reduce the life of electronic equipment [1], machines and mechanisms [2].

Theoretical studies of the effect of external vibration parameters on the dynamic characteristics of structural elements of radio-electronic means (REM) are demonstrated in [3]. A technique for resource prediction of electro-radioelements of a printing unit in conditions of external vibrational effects is stated in [4]. A device for investigating the influence of inertial and deformation components of an external vibration action is described in [5]–[7]. At present, the technologies for active vibration protection of products of radio-electronic equipment are rapidly developed. An information technology presented in [7] ensures the stability of electronic means to external vibration effects. A technique for carrying out testing of electronic means on resistance to external vibrating effects, taking into account their design features, is stated in [8]. The methodological basis for simulating the radiation of a parabolic antenna with allowance for vibrational effects is presented in [9]. A practical technique for such a simulation is presented in [10]. Computational processes for digital modeling of vibrations of complex structures are described in [11].

In fact, all these publications are devoted to the same urgent problem, namely, the problem of analysing the influence of vibration effects on the reliability of various products. They do not affect measurement of vibration parameters. But the analysis of these publications shows that there is a need to create economical and accurate systems for measuring vibration parameters operating in a wide frequency range.

Methods for measuring vibration parameters are divided into contact and non-contact ones. The contact methods include, in particular, piezoelectric, tensometric, and fiber-optic methods. The use of contact vibrometry for measuring the vibration of electronic equipment is limited by the obligatory presence of the contact mass of the sensor, which reduces the sensitivity of the measuring system. Moreover, the higher the frequency of vibration is, the lower the sensitivity of the system is. Contact

\* Corresponding author's e-mail: Jurijs.Lavendels@rtu.lv

measurement of vibrations, which frequency exceeds 2 kHz, is no longer possible.

The known non-contact methods for measuring vibration parameters are divided into methods of laser interferometry, laser Doppler vibrometry, and methods using the analysis of traces of vibrational blurring of images. The first two groups of methods require the use of bulky expensive equipment.

The methods for analysing traces of vibrational blurring of images include, in particular, the use of groups of parallel strokes [12].

The drawbacks of this method include the fact that the vibrational movement of the stencil is fixed exclusively in the plane perpendicular to the optical axis of the recording device. In the process of controlling the vibrations of printed units of radio-electronic equipment, it is often necessary to measure the amplitude of the vibrational displacement of the material points of the printing unit in a direction perpendicular to the plane of the printed circuit board. To solve this problem by these methods, one will have to install another board on the printed circuit board, the plane of which should be located perpendicular to the printed circuit board of the monitored printing unit, and apply a stencil on this board in the form of groups of parallel strokes. The recording device should be positioned in such a way that its optical axis passes perpendicular to the plane of the screen, and parallel to the plane of the printed circuit board of the monitored printing unit. Such a solution is cumbersome and hardly applicable. It will inevitably distort the picture of the vibrational displacements of the material points of the monitored printing unit. Another important disadvantage of these methods is the inability to determine the direction of vibration.

A promising method is the measurement of the vibrational displacement based on the blurring analysis of a round mark image. The essence of this method is that a round mark is placed on the surface of the control object. The image of this mark is registered, a digital photo or video camera being a recording device.

The method makes it possible to measure not only the magnitude, but also the direction of the vibrational displacement of the material point under study. This is due to the fact that the image of the round mark is blurred (due to vibration). The projection of the vector of the vibrational displacement onto the plane of the object (abscissa and ordinate of the vector) is judged by the direction of this blur [13], [14].

In addition, the method uses the effect of defocusing the round mark image, when the original is approached to the recording device, or when it is moving away from it. This factor makes it possible to measure the projection of the vector of the vibrational displacement of the investigated material point onto the axis drawn through the geometric centre of the round mark perpendicular to the plane of the object (i.e., the applicator of this vector).

As a result, the mark can be applied directly to the printed circuit board or to the elements of the printing unit, and the recording device can be arranged so that its optical axis is perpendicular to the plane of the printed circuit board. It is possible to place several marks on the monitoring object in

order to simultaneously measure the vibrational displacement of several points that the recording device keeps in view. A variant of scanning a monitoring object is possible by mechanically moving the recording device.

The patent [15]–[17] proposes a method for measuring the amplitude and direction of the vibrational displacement of the material point under study at the surface of a test object using an analysis of the vibrational blurring of a round mark image, which has a faster response time than the methods presented in [13], [14].

In [16]–[18], it is shown that the measurement signal for the displacement of the material point under study along the applicator is the increment of the radius of the mark blurred due to vibration of the image with respect to the radius of its clear image, previously obtained in the absence of vibration.

### III. A MODEL OF FORMATION AND TRANSFORMATION OF THE MARK IMAGE

In static approaching of the mark to the recording device, the radius of its image increases. This is due to the image defocusing effect. In static removal of the mark from the recording device, the radius of its image decreases due to the same effect.

In the process of vibrational displacement, the mark either approaches the recording device or it is removed from it (Fig. 1).

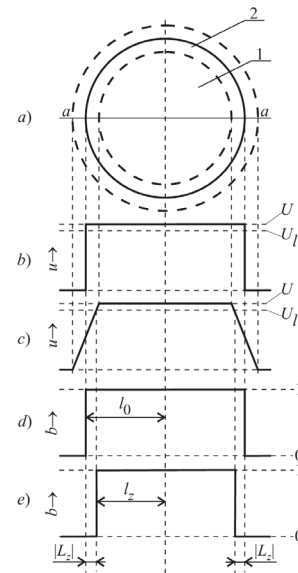


Fig. 1. A model of formation and transformation of the mark image.

In Fig. 1a, the contour of the mark image at the starting position in the absence of vibration is shown with a solid line, and the contours of the defocused mark images in the extreme positions of the vibrational displacement are shown with dotted lines.

Figure 1b shows the intensity distribution of the recorded radiation along the diametrical cross-section of the *a-a* mark image in the absence of vibration; *u* is the current intensity value of the recorded radiation; *U* is the maximum intensity value of the recorded radiation *u*, corresponding to the clear mark image

previously obtained in the absence of vibration;  $u_l$  is the binarization threshold.

Figure 1c shows the intensity distribution of the recorded radiation along the diametrical cross-section of the  $a$ - $a$  mark image in the presence of vibration.

Figure 1d shows the intensity distribution of the binary mark image along the  $a$ - $a$  diametrical cross-section of its halftone image in the absence of vibration;  $b$  is the current level of the binary image;  $l_0$  is the radius of the mark image in the absence of vibration.

Figure 1e shows the intensity distribution of the binary mark image along the  $a$ - $a$  diametrical cross-section of its halftone image in the presence of vibration;  $l_z$  is the radius of the mark image in the presence of vibration;  $|L_z|$  is the absolute value of the radius increment of the mark image caused by vibration.

The greater part of the exposure time the point of the receiving matrix of the recording device is exposed to the influence of a light stream reflected from the mark, the greater intensity of the recorded radiation will be accumulated by the end of the exposure time.

Area 1 of the mark image in the presence of vibration located inside of the internal dotted line (Fig. 1a) is constantly exposed to the stream mark reflected from the light, and area 2 of the mark image located between the inner and outer dotted lines is exposed to this light stream only part of the exposure time. Moreover, this part is smaller, if the distance is greater from the area point of the image between the two dashed lines to the centre of gravity of the mark image. Therefore, the intensity of the recorded radiation in area 2 decreases with the distance from the centre of gravity of the blurred mark image (Fig. 1c).

The first step in deciding whether a pixel belongs to the mark image is the binarization of the original halftone image, i.e., an assignment to each pixel either a logical zero level or a logic unit level. At the simplest binarization, the logical unit level is assigned to the pixel, if the intensity of the recorded radiation in this pixel exceeds a certain level, called the binarization threshold [18]–[20].

As it can be seen from Fig. 1e and Fig. 1d, if the binarization threshold level is higher than  $U/2$ , then the radius of the blurred image will be less than the radius of the clear image. The greater vibrational displacement is, the higher the blurred level and, consequently, the larger, in absolute value, the difference between the radius of the blurred and clear image is. It is this absolute value of the difference  $|L_z|$  between the radius of blurred and clear images of the mark that is the measuring signal of the vibrational displacement of the material point under study.

#### IV. THE LIMITING ABSOLUTE ERROR OF THE MEASURING SIGNAL

Measurement of the absolute difference value  $|L_z|$  between the radius of the blurred and clear mark images is indirect, for which calculations based on direct area measurements of the two mark images are performed: the clear one in the absence of vibration and the blurred one when there is vibration. These

measurements consist in counting of the pixel number belonging to the mark image:

$$S_{imt} = \sum_{i=1}^I \sum_{j=1}^J \xi_{imt}(i, j), \quad (1)$$

where  $S_{imt}$  is the mark image area, measured in  $run^2$ ;  $i$  and  $j$  are the sequence numbers, respectively, lines and matrix column of the digital raster image at the intersection of which the pixel is located;  $I, J$  are the numbers of lines and columns of the scanned matrix of the digital raster image, respectively;  $\xi_{imt}$  is the function that takes a value equal to 1  $run^2$  if the pixel with discrete coordinates  $(i, j)$  belongs to the mark image, and is equal to zero, otherwise.

$$S_{imt0} = \sum_{i=1}^I \sum_{j=1}^J \xi_{imt0}(i, j), \quad (2)$$

where  $S_{imt0}$  is the clear mark image area obtained in the absence of vibration, measured in  $run^2$ ;  $\xi_{imt0}$  is the function that takes a value equal to 1  $run^2$  if the pixel with discrete coordinates  $(i, j)$  belongs to the clear mark image obtained in the absence of vibration, and is equal to zero, otherwise.

$$S_{imtz} = \sum_{i=1}^I \sum_{j=1}^J \xi_{imtz}(i, j), \quad (3)$$

where  $S_{imtz}$  is the blurred mark image area obtained in the presence of vibration, measured in  $run^2$ ;  $\xi_{imtz}$  is the function that takes a value equal to 1  $run^2$  if the pixel with discrete coordinates  $(i, j)$  belongs to the blurred mark image obtained in the presence of vibration, and is equal to zero, otherwise.

The radius  $r_{imt}$  of the mark image is calculated by the formula:

$$r_{imt} = \sqrt{\frac{S_{imt}}{\pi}}. \quad (4)$$

Hence,

$$l_0 = \sqrt{\frac{S_{imt0}}{\pi}}, \quad (5)$$

where  $l_0$  is the radius of the clear mark image obtained in the absence of vibration

$$l_z = \sqrt{\frac{S_{imtz}}{\pi}}, \quad (6)$$

where  $l_z$  is the radius of the blurred mark image obtained in the presence of vibration.

Based on these measurements and calculations, a measuring signal  $|L_z|$  is calculated:

$$|L_z| = |l_z - l_0|, \quad (7)$$

where  $|L_z|$  is the absolute value of the difference between the radius of two images of the mark: the clear one, obtained in the absence of vibration, and the blurred one, obtained in the presence of vibration.

The source of the measurement error of the mark image area  $S_{imt}$  is the conversion of the continuous mark image into a discrete one by the recording device (Fig. 2).

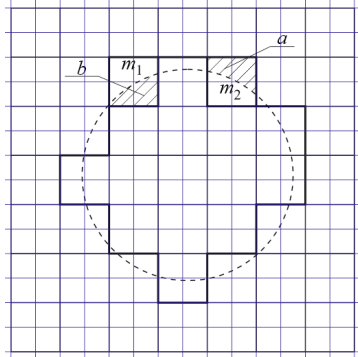


Fig. 2. A model for discretization of the round mark image.

A pixel located on the periphery of a true continuous mark image is included in the registered discrete mark image, if most part of its area belongs to a continuous mark image, and is not included, otherwise. And the smaller part of the pixel, which in the first case is not included in the mark image, but is included in the second case, is the elementary error of discretization of the mark image. In Fig. 2, the elementary errors of the discretization of the mark image introduced by a and b pixels are shaded. The elementary discretization error of the mark image has a plus sign, if it is included in the registered discrete mark image, and a minus sign, otherwise. The elementary discretization error of the mark image  $\epsilon_{pix}$  is a random variable, evenly distributed in the range from minus  $0.5 run^2$  to  $0.5 run^2$ . Here it is the dispersion formula of the uniformly distributed random variable:

$$D(\epsilon_{pix}) = \frac{(\epsilon_{pixU} - \epsilon_{pixL})^2}{12}, \quad (8)$$

where  $D(\epsilon_{pix})$  is the dispersion of the random variable  $\epsilon_{pix}$ ;  $\epsilon_{pixU}$  and  $\epsilon_{pixL}$  are upper and lower bounds of the error  $\epsilon_{pix}$ , respectively;  $\epsilon_{pixU} = 0.5 run^2$ ,  $\epsilon_{pixL} = -0.5 run^2$ . Hence,  $D(\epsilon_{pix}) = (1/12) run^4$ . The measurement error of the mark image area is equal to the sum of the elementary discretization errors of this image introduced by the pixels located on the periphery of the true continuous mark image.

The number of such pixels is equal to the circumference of the continuous mark image divided by the expected value of arc length of this circle located within the pixel (Fig. 2):

$$N_{pit} = \frac{L_{imt}}{M(l_{pix})}, \quad (9)$$

where  $N_{pit}$  is the number of peripheral pixels of the mark image;  $L_{imt}$  is the circumference of the true continuous mark image;

$M(l_{pix})$  is mathematical expectation of the arc length of the circle of the continuous mark image located within the pixel.

The length  $l_{pix}$  of the arc of the circle of the continuous mark image located within the pixel is a random variable uniformly distributed from zero to  $2^{1/2}run$  (Fig. 2). It follows that  $M(l_{pix}) = (2^{1/2}/2)run$ . The circumference of a true continuous mark image is:

$$L_{imt} = 2\pi r_{imt}. \quad (10)$$

Using (9) and (10), and taking into account that  $M(l_{pix}) = (2^{1/2}/2)run$ :

$$N_{pit} = 2\sqrt{2}run^{-1}\pi r_{imt}. \quad (11)$$

Further, using (4):

$$N_{pit} = \sqrt{8run^{-2}\pi S_{imt}}. \quad (12)$$

The absolute area measurement error of the mark image will be determined as the algebraic sum of the elementary errors of the mark image discretization. Dispersion of the sum of random variables is equal to the sum of their dispersions. It follows that:

$$D(S_{imt}) = D(\epsilon_{pix})N_{pit}. \quad (13)$$

Thus, using (12) and taking into account that  $D(\epsilon_{pix}) = (1/12)run^4$ :

$$D(S_{imt}) = \sqrt{\frac{1}{18}run^6\pi S_{imt}}. \quad (14)$$

Mean square deviation of the measured value  $S_{imt}$ :

$$\sigma(S_{imt}) = \sqrt[4]{\frac{1}{18}run^6\pi S_{imt}}. \quad (15)$$

Since the measurement error  $S_{imt}$  is the sum of a large number of elementary uniformly distributed errors  $\epsilon_{pix}$ , according to the law of large numbers, this error itself is distributed according to the normal law.

If some random variable  $X$  is distributed according to the normal law, then the probability that its value is within  $X \pm 3\sigma(X)$  exceeds 0.997. It follows that the measured  $S_{imt}$  value with a confidence probability of 0.997 is within  $S_{imt} \pm \Delta S_{imt}$ , where  $\Delta S_{imt} = 3\sigma(S_{imt})$ . The value  $\Delta S_{imt}$  is the limiting absolute area measurement error of the mark image.

Upper  $S_{imtU}$  and lower  $S_{imtL}$  interval bounds of the value coverage  $S_{imt}$ :

$$S_{imtU} = S_{imt} + \Delta S_{imt}. \quad (16)$$

$$S_{imtL} = S_{imt} - \Delta S_{imt}. \quad (17)$$

Taking into account (15) and the fact that  $\Delta S_{imt} = 3\sigma(S_{imt})$ :

$$\Delta S_{imt} = \sqrt[4]{4.5run^6 \pi S_{imt}}. \quad (18)$$

It follows from (4) that:

$$r_{imtU} = \sqrt{\frac{S_{imtU}}{\pi}}. \quad (19)$$

$$r_{imtL} = \sqrt{\frac{S_{imtL}}{\pi}}. \quad (20)$$

where  $r_{imtU}$  and  $r_{imtL}$  are, respectively, the upper and lower interval bounds for the coverage of the radius values of the mark image  $r_{imt}$ .

Hence,

$$l_{0U} = \sqrt{\frac{S_{imt0U}}{\pi}}, \quad (21)$$

$$l_{0L} = \sqrt{\frac{S_{imt0L}}{\pi}}, \quad (22)$$

where  $l_{0U}$  and  $l_{0L}$ ,  $S_{imt0U}$  and  $S_{imt0L}$  are, respectively, the upper and lower intervals bounds of the value coverage  $l_0$  and  $S_{imt0}$ .

$$l_{zU} = \sqrt{\frac{S_{imtzU}}{\pi}}, \quad (23)$$

$$l_{zL} = \sqrt{\frac{S_{imtzL}}{\pi}}, \quad (24)$$

where  $l_{zU}$  and  $l_{zL}$ ,  $S_{imtzU}$  and  $S_{imtzL}$  are, respectively, the upper and lower intervals bounds of the value coverage  $l_z$  and  $S_{imtz}$ .

It follows from (7) that:

$$|L_z|_U = \begin{cases} l_{zU} - l_{0L}, & \text{if } l_z \geq l_0, \\ l_{0U} - l_{zL}, & \text{if } l_z < l_0 \end{cases}, \quad (25)$$

where  $|L_z|_U$  and  $|L_z|_L$  are, respectively, the upper and lower interval bounds of the value coverage  $|L_z|$ .

The limiting absolute error  $\Delta|L_z|$  of measuring signal is determined by:

$$|L_z|_L = \begin{cases} l_{zL} - l_{0U}, & \text{if } (l_z \geq l_0) \cap (l_{zL} \geq l_{0U}) \\ 0, & \text{if } (l_z \geq l_0) \cap (l_{zL} < l_{0U}) \\ l_{0L} - l_{zU}, & \text{if } (l_z < l_0) \cap (l_{0L} \geq l_{zU}) \\ 0, & \text{if } (l_z < l_0) \cap (l_{0L} < l_{zU}) \end{cases}. \quad (26)$$

$$\Delta|L_z| = \begin{cases} |L_z|_U - |L_z|_L, & \text{if } |L_z|_U - |L_z|_L \geq |L_z|_U - |L_z|_L, \\ |L_z|_L - |L_z|_U, & \text{if } |L_z|_L - |L_z|_U < |L_z|_U - |L_z|_L \end{cases}, \quad (27)$$

i.e., the greatest deviation of the measured radius increment of the mark image from the true by the absolute value is assumed as the limiting absolute error of the measuring signal.

## V. THE REDUCED ERROR OF MEASURING TRANSFORMATION

To evaluate the possibilities of measuring transformation, the concept of the reduced error of this transformation is used. The standard [17] determines the reduced error of the measuring transformation as the ratio of the limiting absolute error of the measuring transformation to the normalizing value of the measured quantity.

With reference to this measuring transformation, this means:

$$\delta_N M = \frac{\Delta M(M_N)}{M_N}, \quad (28)$$

where  $\delta_N M$  is the reduced error of the measuring transformation of the vibrational displacement of the material point under study to the absolute value of the radius increment of the round mark image applied to the surface of the test object;  $M_N$  is the normalizing value of the vibrational displacement;  $\Delta M(M_N)$  is the limiting absolute error of the measuring transformation under the vibrational displacement of the material point under study  $M$  equal to  $M_N$ .

If the dependence of the measuring signal  $|L_z|$  on the measured value  $M$  is linear, then:

$$\frac{\Delta|L_z|}{|L_z|} = \frac{\Delta M}{M},$$

or

$$\frac{\Delta|L_z|(M_N)}{|L_z|(M_N)} = \frac{\Delta M(M_N)}{M_N},$$

where  $|L_z|(M_N)$  and  $\Delta|L_z|(M_N)$  are, respectively, the absolute value of the radius increment, and the limiting absolute error of its measurement for  $M = M_N$ .

From this and (28), it follows that for a linear calibration characteristic of the measuring transformation, the reduced error of this transformation, expressed in percent, will be:

$$\delta_N M = \frac{\Delta|L_z|(M_N)}{|L_z|(M_N)} \cdot 100\%. \quad (29)$$

An important characteristic of this measuring transformation is the relative radius increment of the round mark image with the normalizing value of the vibrational displacement of the material point under study  $L_{zrel}(M_N)$ :

$$L_{zrel}(M_N) = \frac{l_z(M_N)}{l_0} \cdot 100\%. \quad (30)$$

Knowing the mark image area  $S_{imt0}$  in the absence of vibration and the relative radius increment of the round mark image with the normalizing value of the vibrational displacement of the material point under study  $L_{zrel}(M_N)$ , it is possible to calculate the reduced measurement error of the vibrational displacement  $\delta_N M$ . To do this, first it is necessary to calculate the radius of

the mark image  $l_0$  in the absence of vibration by (5). Then it is necessary to calculate the radius increment of the mark image with the normalizing value of the vibrational displacement of the material point under study  $L_z(M_N)$ :

$$L_z(M_N) = \frac{L_{zrel}(M_N)l_0}{100\%}. \quad (31)$$

Formula (31) is obtained as a solution of (30).

Based on the known  $l_0$  and  $L_z(M_N)$ , the radius of the mark image is calculated at the normalizing value of the vibrational displacement  $l_z(M_N)$ :

$$l_z(M_N) = l_0 + L_z(M_N). \quad (32)$$

The area of the mark image with the normalizing value of the vibrational displacement is calculated by the formula:

$$S_{imz}(M_N) = \pi l_z^2(M_N). \quad (33)$$

The limiting absolute errors  $\Delta S_{im0}$  and  $\Delta S_{imz}(M_N)$  are calculated on the basis of (18):

$$\Delta S_{im0} = \sqrt[4]{4.5run^6 \pi S_{im0}}, \quad (34)$$

$$\Delta S_{imz}(M_N) = \sqrt[4]{4.5run^6 \pi S_{imz}(M_N)}. \quad (35)$$

The interval bounds of the value coverage for  $S_{im0}$  and  $S_{imz}(M_N)$  are calculated using (16) and (17):

$$S_{im0U} = S_{im0} + \Delta S_{im0}. \quad (36)$$

$$S_{im0L} = S_{im0} - \Delta S_{im0}. \quad (37)$$

$$S_{imzU}(M_N) = S_{imz}(M_N) + \Delta S_{imz}(M_N). \quad (38)$$

$$S_{imzL}(M_N) = S_{imz}(M_N) - \Delta S_{imz}(M_N). \quad (39)$$

Then, by means of successive calculations using (21–27, 29), the reduced measurement error of the vibrational displacement of the material point under study at the control object surface  $\delta_N M$  is determined.

The dependence of  $\delta_N M$  on  $S_{im0}$  is made by sequentially value setting  $S_{im0}$  in a certain range with a certain step, and calculating  $\delta_N M$  by the method described.

Based on this dependence, knowing the field of view area of the recording device, its resolving power and the diameter of the round mark, it is possible to determine the mark image area and the reduced measurement error; or, conversely, by setting the required reduced error, to select the recording device, its field of view area, and the diameter of the mark. This also applies to the variant in which not a single mark is applied to the surface area of the monitoring object, but a matrix of marks, to distribution control of the vibrational displacements of material points in this section of the monitoring object.

## VI. THE RESULTS OF EXPERIMENTAL STUDIES

Figure 3 depicts a scheme of the experiment conducted by the authors.

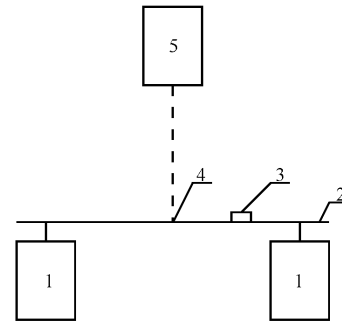


Fig. 3. An experiment scheme of a measurement system graduation of vibrational displacement.

Circuit board 2 was placed on vibration exciters 1, where a mechanical contact sensor of vibration acceleration 3 was fixed, and a round white mark 4 with a diameter of 4 mm was plotted on a black background. A recording device, a digital light-optical microscope *DigiMicroProf*, was placed above this mark. The camera resolution is 5 Mpix. First, the photographing of the mark was carried out in the absence of vibration (Fig. 4a).

The resulting photograph was exposed to binarization with a threshold level  $u_l = 0.9U$ , and to filtering with the aim to eliminate white inclusions outside the mark image, and black holes inside this image.

In line reading of binary filtered image, counting of the number of pixels was carried out belonging to the mark image by (2), as a result of which the area of the round mark image  $S_{im0}$  was measured in the absence of vibration. Based on this result, the radius of the mark image was calculated by (5) in the absence of vibration  $l_0$ .

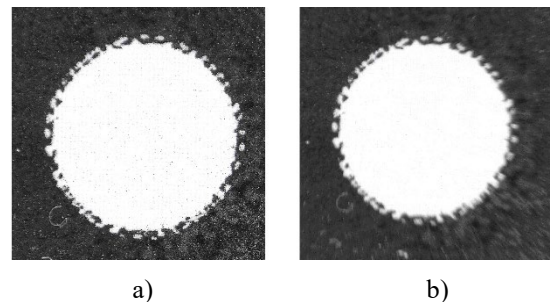


Fig. 4. An original half-tone image of the round mark: a) in the absence of vibration; b) in the presence of vibration.

Then the vibration was excited. The vibration was regulated by the indications of a contact sensor: harmonic vibrations of frequency 50 Hz, and vibration acceleration amplitude  $1g, 2g, \dots, 9g$  was successively formed, where  $g$  is the acceleration of gravity.

Figure 4b shows the initial half-tone round mark image with the maximum experimental vibration of  $9g$ .

For each value of the vibration acceleration amplitude measured in  $g$  units, the corresponding value of the vibrational

displacement measured in micrometers was calculated. Since harmonic vibrations are formed by means of simple mathematical transformations, the following formula is obtained:

$$M[\mu m] = \frac{10^6 A \cdot g}{(2\pi f)^2}, \quad (40)$$

where  $M$  [ $\mu m$ ] is the amplitude of the vibrational displacement, measured in micrometers;  $A$  is the vibration acceleration amplitude, measured in  $g$  units ( $1g, 2g, \dots, 9g$ );  $g$  is acceleration of gravity assumed to be  $9.807 \text{ m/s}^2$ ;  $f$  is the vibration frequency, Hz.

At each value of the vibration acceleration, the recording device carried out fixation of the mark image. This image underwent binarization with a threshold level  $u_t = 0.9U$ . The resulting binary image underwent filtration to remove parasitic white inclusions of a black background, and to remove black holes inside the binary image of the white mark. Counting of the pixel number belonging to the blurred mark image was carried out by (3), as a result of which the area values of the blurred mark images  $S_{imz}(k)$  were formed, where  $k$  is the sequence number of the mark image obtained in the presence of vibration. For each  $k$  value, the radius  $l_z(k)$  of the filtered binary mark image, measured in raster units  $run$ , was determined by (6). The values of the radius increment of the mark image caused by the vibrational displacement of the material point under study were calculated from the formula:

$$L_z(k) = l_z(k) - l_0, \quad (41)$$

where  $L_z(k)$  is the radius increment of the  $k$ -th blurred mark image caused by the vibrational displacement of the material point under study. The results of these measurements are presented in Table I.

TABLE I  
THE RESULTS OF MEASUREMENTS

$S_{im0} = 739219run^2; l_0 = 485.078run$					
$k$	$A(k), g$	$M(k), \mu m$	$S_{imz}(k), run^2$	$l_z(k), run$	$L_z(k), run$
1	1	99.37	735973	484.012	-1.06619
2	2	198.7	735889	483.984	-1.09381
3	3	298.1	734623	483.568	-1.51031
4	4	397.5	733192	483.097	-1.98152
5	5	496.8	731341	482.486	-2.59171
6	6	596.2	729387	481.841	-3.23669
7	7	695.6	729112	481.751	-3.32754
8	8	794.9	727353	481.169	-3.90901
9	9	894.3	726479	480.880	-4.19818

VII. DEPENDENCE OF THE MEASURING SIGNAL ON THE MEASURED VALUE

Figure 5 shows the experimental dependence graph of the measuring signal, the absolute value of the radius increment of the mark image  $|L_z|$ , measured in raster units, on the amplitude of the vibrational displacement of  $M$  mark, measured in micrometers.

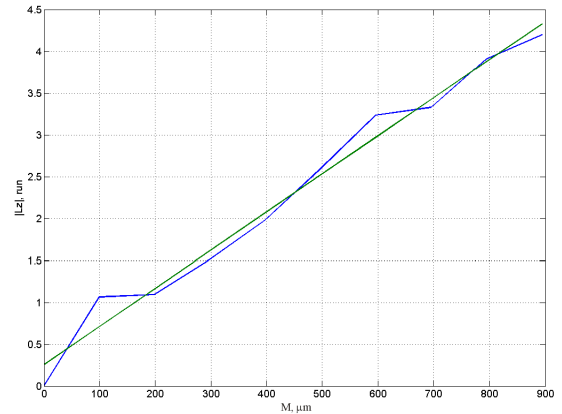


Fig. 5. An experimental dependence of the absolute value of the radius increment of the round mark image on the vibrational displacement of the investigated material point.

The experimental dependence was approximated by a straight line using the method of least squares. An analysis of the graph shows that the obtained calibration characteristic of the measuring transformation can be considered to be a linear one.

As a normalizing vibrational displacement of the material point under study, it is convenient to take the value  $M_N = 1000 \mu m$ . Extrapolation of the approximating straight line gives the result:  $|L_z|(M_N) = 4.80838 run$ . Taking into account the fact that in this experiment  $l_z < l_0$ :  $L_z(M_N) = 4.80838 run$ . The experimental radius value of the mark image in the absence of vibration  $l_0$  is given in Table I. The experimental value of the mark image area  $S_{im0}$  in the absence of vibration is also given there. Sequential calculations according to (32–39, 21–27, and 29) lead to the result: the reduced measurement error  $\delta_N M$  with the normalizing vibrational displacement  $M_N = 1000 \mu m$  is 0.777869 %.

VIII. THE REDUCED MEASUREMENT ERROR OF VIBRATIONAL DISPLACEMENT OF AN INVESTIGATED MATERIAL POINT AS A FUNCTION OF PIXEL NUMBER OF THE ROUND MARK IMAGE

The relative radius increment of the round mark image with the normalizing value of the vibrational displacement of the investigated material point  $L_{zrel}(M_N)$  is determined by (30). For the experiment conditions presented in clause 7, this parameter is 0.991259 %.

Based on the experimental data, a function of the reduced measurement error of the vibrational displacement is obtained by means of successive calculations using (31–39, 21–27, and 29). Its argument is the pixel number per mark image, i.e., the mark image area in the absence of vibration, expressed in  $run^2$  (Fig. 6).

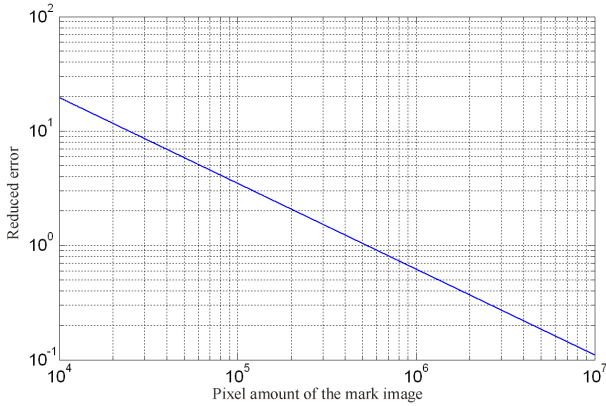


Fig. 6. The reduced measurement error of vibrational displacement as a function of the round mark image area.

IX. FORECASTING OF THE REDUCED ERROR IN VIBRATIONAL DISPLACEMENT MEASUREMENT OF THE INVESTIGATED MATERIAL POINT

Figure 7 shows a model of the round mark image with a diameter of 4 mm, and a 6 mm raster height of the recording device.

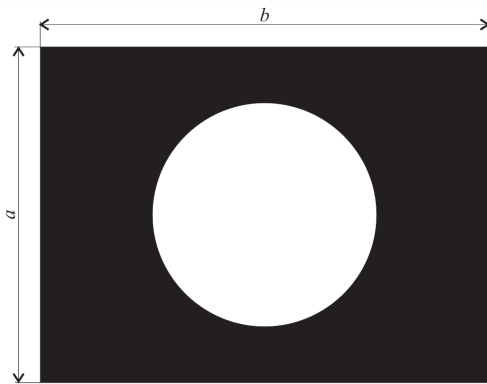


Fig. 7. A model of the round mark image.

The mark is linearly projected onto the photosensitive surface of the recording device, and, as a result, a continuous image of the mark is formed on this surface, being exposed to discretization by a photo receiving matrix of the recording device. It follows from the linear character of the projection, that:

$$\frac{S_f}{S_t} = \frac{S_{gim}}{S_{imi}}, \tag{42}$$

where  $S_f$  is the field of view area of the camera, measured in  $mm^2$ ;  $S_t$  is the area of the original mark, measured in  $mm^2$ ;  $S_{gim}$  is the area of the entire raster image, measured in  $run^2$ ;  $S_{imi}$  is the area of the mark image, measured in  $run^2$ .

Hence,

$$S_{imi} = \frac{S_t \cdot S_{gim}}{S_f}. \tag{43}$$

The area of the original mark is determined by:

$$S_t = \frac{\pi d_t^2}{4}, \tag{44}$$

where  $d_t$  is the diameter of the original mark, measured in mm (Fig. 7).

The camera field of view area  $S_f$ , measured in  $mm^2$ , is determined as the product of its width  $a$ , and its length  $b$  (Fig. 7):

$$S_f = ab. \tag{45}$$

Based on the principle of similarity of the field of view of the recording device, and the raster image formed by it, it follows that:

$$\frac{a}{b} = f_r, \tag{46}$$

where  $f_r$  is the ratio of the line number of the photo receiving matrix of the recording device to the number of its columns.

A comparison of (43–46) results in obtaining the calculation for  $S_{imi0}$ :

$$S_{imi0} = \frac{\pi d_t^2 f_r S_{gim}}{4a^2}. \tag{47}$$

If, for example, a recording device is a camera with a resolution of 5 Mpix, then the area of the entire raster image is  $S_{gim} = 5 \cdot 10^6 run^2$ . If, in this case,  $a = 6 mm$ , and  $f_r = 0.75$ , then the calculation by (47) will show that  $S_{imi0} = 1.30900 \cdot 10^6 run^2$ . Sequential calculations using (5, 31–39, 21–27, and 29) will show that the reduced measurement error of vibrational displacement of the investigated material point  $\delta_N M$  at the normalizing value of  $1000 \mu m$  is 0.506737 %.

Thus, using a camera with a resolution of 5 Mpix, the presented technique allows measuring the vibrational displacement of the investigated material point if the reduced measurement error at normalizing value of the measured value of  $1000 \mu m$  is not more than 0.51 %.

X. CALCULATION OF PARAMETERS OF THE FIELD OF VIEW OF THE RECORDING DEVICE FOR A GIVEN MAXIMUM VALUE OF THE REDUCED MEASUREMENT ERROR OF THE VIBRATIONAL DISPLACEMENT OF EACH INVESTIGATED MATERIAL POINTS

The technique for vibrational displacement measurement of the investigated material point proposed in this article provides the possibility of simultaneous measurement of the vibrational displacements of several material points located in the field of view of the recording device, i.e., the possibility of measurement of the distribution parameters of the vibrational

displacement on the flat surface of the monitoring object. To solve this problem, a grid of round marks, having the same diameter, is applied to the flat surface of the monitoring object (Fig. 8).

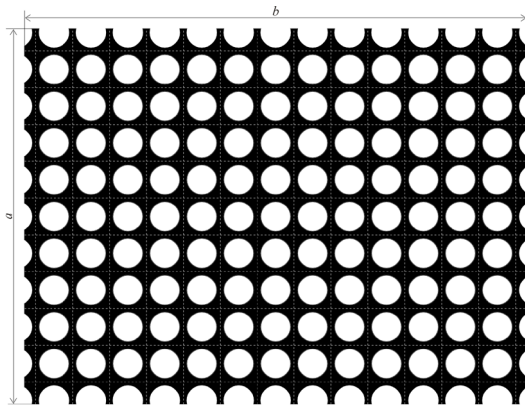


Fig. 8. A matrix of round marks in the field of view of the recording device.

Let us, for example, calculate the maximum width  $a_{max}$  and the length  $b_{max}$  of the field of view of the recording device, in which it is possible to measure the amplitudes of the vibrational displacements of the investigated material points with a reduced error not exceeding a certain limiting value  $\delta_{Nmax}M$ . In this case, the normalizing value of the vibrational displacement of the investigated material point  $M_N$ , the diameter of the mark  $d_t$ , the resolution possibility of the recording device  $S_{gim}$ , and the ratio of the line number of the photo receiving matrix of the recording device to the number of its columns  $f_r$  are given.

The maximum width of the field of view of the recording device is defined as the solution of (47):

$$a_{max} = d_t \sqrt{\frac{\pi f_r S_{gim}}{4 S_{imt0min}}} \quad (48)$$

The area of the mark image  $S_{imt0min}$  in the absence of vibration will be determined based on the function of the reduced error of the measurement transformation similar to that shown graphically in Fig. 6.

The length  $b_{max}$  of the field of view of the recording device is calculated from the formula obtained on the basis of (46):

$$b_{max} = \frac{a_{max}}{f_r} \quad (49)$$

If, for example, the maximum reduced measurement error  $\delta_{Nmax} M = 5\%$  is specified with the normalizing vibrational displacement of the investigated material point  $M_N = 1000 \mu m$ , the mark diameter is  $d_t = 4 \text{ mm}$ . The camera with a resolution of 5 Mpix and with a standard height ratio of the receiving raster to its width of 3×4 is used as a recording device.

To solve this problem, first it is necessary to determine the minimum area of the mark image  $S_{imt0min}$  in the absence of vibration, sufficient to satisfy the condition  $\delta_N M \leq 5\%$ .  $S_{imt0min}$  is

found from Table II, obtained from the function analysis of the reduced measurement error, graphically presented in Fig. 6.

TABLE II  
A FRAGMENT OF THE REDUCED ERROR FUNCTION TO MEASURE THE VIBRATION DISPLACEMENT AMPLITUDE

$S_{im0}, \text{run}^2$	61700	61800	61900	62000	62100
$\delta_N M, \%$	5.00925	5.00317	4.99711	4.99106	4.98503

Table II shows that it is better to take the value  $S_{im0min} = 61900 \text{ run}^2$ . Since the camera with a resolution of 5 Mpix and with a standard height ratio of the receiving raster to its width of 3×4 is used as a recording device, then  $S_{gim} = 5 \cdot 10^6 \text{ run}^2$ ,  $f_r = 0.75$ . The diameter of the mark is  $d_t = 4 \text{ mm}$ . By (48),  $a_{max} = 27.5915 \text{ mm} \approx 28 \text{ mm}$ . By (49)  $b_{max} = 36.7887 \text{ mm} \approx 37 \text{ mm}$ .

Thus, the presented technique allows using a camera with a resolution of 5 Mpix to measure the distribution of the vibrational displacement on a portion of a flat surface of a test object with dimensions of 28×37 mm. The reduced measurement error at a normalizing value of the measured value of 1000 μm does not exceed 5%.

A new technology for vibration measurement is formulated, for realization of which a matrix of round marks is applied to the surface of the object; a recording device forms images of this matrix in the absence of vibration, and in its presence; the absolute value of the difference between the radius of the blurred mark image is applied as a measuring signal, obtained in the presence of vibration, and its clear image obtained in the absence of vibration. The radius measurement of the round mark image is indirect: first, by pixel counting belonging to the mark image, the area of this image is measured, and then the radius is calculated. In the article, a function connecting the reduced error of the given measurement transformation with the number of pixels per mark image is revealed for the first time.

The results of experimental studies proving the linearity of the measurement transformation and establishing a relative radius increment of the mark image at the normalizing level of the vibrational displacement of the investigated material point are presented.

The numerical examples show the conditions for resolving the technical contradiction between the dimensions of the control area and the accuracy of the measurements.

#### ACKNOWLEDGMENT

The research has been conducted at the expense of the grant of the Russian Science Foundation (the project No. 17-79-10281 as of 24 July 2017).

#### REFERENCES

- [1] R. C. Gonzalez and R. E. Woods, *Digital image processing*. New Jersey, USA: Prentice Hall, 2008.
- [2] G. V. Tankov, S. A. Brostislov, N. K. Yurkov and A. V. Lysenko, "Information-measuring and operating systems to test for the effects of vibration," in *2016 International Siberian Conference on Control and Communications*, SIBCON, May 2016. <https://doi.org/10.1109/SIBCON.2016.7491679>

- [3] P. H. Rogers and H. M. Cox, "Noninvasive vibration measurement system and method for measuring amplitude of vibration of tissue in an object being investigated," *The Journal of the Acoustical Society of America*, vol. 86, no. 5, 1989. <https://doi.org/10.1121/1.398507>
- [4] I. I. Kochegarov, E. A. Danilova, N. K. Yurkov, P. Y. Bushmelev, and A. M. Telegin, "Analysis and modeling of latent defects in the printed conductors," in *2016 13th International Scientific-Technical Conference on Actual Problems of Electronics Instrument Engineering (APEIE)*, Novosibirsk, Russia, October 03–06, 2016. <https://doi.org/10.1109/APEIE.2016.7806897>
- [5] A. V. Grigorev, A. K. Grishko, N. V. Goryachev, N. K. Yurkov, and A. M. Mischev, "Contactless three-component measurement of mirror antenna vibrations," *Proceedings 2016 International Siberian Conference on Control and Communications*, SIBCON, May 2016. <https://doi.org/10.1109/SIBCON.2016.7491673>
- [6] A. K. Grishko, N. V. Goryachev, I. I. Kochegarov, and M. P. Kalaev, "Mathematical models of the system of measurement and analysis of temperature parameters of radio electronic modules," in *2016 13th International Scientific-Technical Conference on Actual Problems of Electronics Instrument Engineering (APEIE)*, Novosibirsk, Russia, October 03–06, 2016. <https://doi.org/10.1109/APEIE.2016.7806424>
- [7] C. Y. Fah, O. M. Rijal and N. M. Noor, "Image quality and noise evaluation, Signal Processing and Its Applications", *Proceedings, Seventh International Symposium*, July 2003. <https://doi.org/10.1109/ISSPA.2003.1224740>
- [8] E. Y. Maksimov, N. K. Yurkov, and A. N. Yakimov, "A finite-element model of the thermal influences on a microstrip antenna," *Measurement techniques*, vol. 54, no. 2, pp. 207–212, May 2011. <https://doi.org/10.1007/s11018-011-9707-y>
- [9] A. V. Dubravin, S. A. Zinkin, and D. V. Paschenko, "Formal and conceptual definitions of the hybrid model of distributed computings in networks," *Proceedings 2015 International Siberian Conference on Control and Communications*, SIBCON, May 2015. <https://doi.org/10.1109/SIBCON.2015.7147047>
- [10] M. Y. Mikheev, V. R. Roganov, P. G. Andreev, N. V. Goryachev, V. A. Trusov, "Developing the structure of the quality control system of power supply units in mobile robots," *Proceedings in 2017 International Siberian Conference on Control and Communications*, SIBCON, June 2017. <https://doi.org/10.1109/SIBCON.2017.7998579>
- [11] M. Zielinski and G. Ziller, "Noncontact vibration measurements on compressor rotor blades," *Measurement Science and Technology*, vol. 11, no. 7, pp. 847–856, 2000. <https://doi.org/10.1088/0957-0233/11/7/301>
- [12] J. Lénárt, "Contactless vibration measurement using linear CCD sensor," *Proceedings of the 13th International Carpathian Control Conference (ICCC)*, High Tatras, Slovakia, pp. 426–429, 2012. <https://doi.org/10.1109/CarpathianCC.2012.6228681>
- [13] V. R. Roganov, E. A. Asmolova, A. N. Seregin, M. V. Chetvergova, N. B. Andreeva, and V. O. Filippenko, "Problem of virtual space modelling in aviation simulators," *Life Science Journal*, 2014. [Online]. Available: <http://www.penzgtu.ru/fileadmin/filemounts/its/staff/publish/filippenko/p3.pdf>
- [14] K. R. McCall, M. Boudjema, I. B. Santos, R. A. Guyer, and G. N. Boitnott, "Nonlinear, hysteretic rock elasticity: Deriving modulus surfaces," *American Rock Mechanics Association DC Rocks*, The 38th U.S. Symposium on Rock Mechanics (USRMS), Washington USA, 7–10 July, 2001.
- [15] D. Herrmann, "Temperature Errors and Ways of Elimination for Contactless Measurement of Shaft Vibrations," *Technisches Messen*, vol. 55, no. 1, 1988.
- [16] W. B. Hemphins, R. H. Kingsborough, W. E. Lohec, and C. J. Nini, "Multivariate statistical analysis of stuck drillpipe situations," *SPE Drilling Engineering*, vol. 2, no. 3, pp. 237–244, 1987. <https://doi.org/10.2118/14181-PA>
- [17] V. S. Padalko and E. A. Zryumov, "Experimental Research of the Effect of the LEDs Brightness on the Structure of the Image of the Dynamic Test Object," in *Proceedings of 13th International Scientific-Technical Conference on Actual Problems of Electronic Instrument Engineering APEIE*, Novosibirsk, Russian Federation, 2016, pp. 299–301. <https://doi.org/10.1109/APEIE.2016.7802281>
- [18] C. Ding, J. L. G. Janssen, A. A. H. Damen, P. P. J. van den Bosch, J. J. H. Pau-lides and E. Lomonova, "Modeling and realization of a 6-DoF contactless elec-tromagnetic anti-vibration system and verification of its static behavior," *2012 IEEE/ASME International Conference on Advanced Intelligent Mechatronics (AIM)*, Kachsiung, Taiwan, August 2012, pp. 149–154. <https://doi.org/10.1109/AIM.2012.6265880>
- [19] E. A. Zryumov, P. A. Zryumov and S. P. Pronin, "Optoelectronic stroboscopic system for measurement of the frequency of harmonic vibrations based on the use of a genetic algorithm," in *Measurement Techniques*, vol. 55, no. 4, pp. 425–430, 2012. <https://doi.org/10.1007/s11018-012-9976-0>
- [20] S. P. Pronin and E. A. Zryumov, "A meter of the double-amplitude peak and frequency of low-frequency harmonic vibrations," in *2010 Instruments and Experimental Techniques*, vol. 53, no. 2, pp. 296–297, 2010. <https://doi.org/10.1134/S0020441210020259>



**Alexey Grigorev** Valeryavich graduated from Penza Polytechnic Institute in the specialty of Design and Manufacture of Radio Equipment in 1981. Research interests include processing and automated analysis of raster images. In 1999, he defended his thesis for the direct registration and processing of electron diffraction patterns. He is a Candidate of Technical Sciences, Associate Professor.

E-mail: a\_grigorev@mail.ru



**Alexey Lysenko** graduated from Penza State University (Penza) in the specialty of Designing and Technology of Electronic Means in 2010. In 2015, he received the diploma about assignment of a scientific degree of candidate of technical sciences. Since 2015, he has been working as an Associate Professor of the Department of Designing and Production of Radio Equipment at Penza State University. Scientific interests are related to development in the areas of space technology concerning the sustainability of the RES to vibration and shock. During scientific and research activities he has published about 100 scientific papers in Russia and abroad. In 2015, he received a grant from the Russian Science Foundation on the theme "Development of Methods and Tools for Building Highly Reliable Components and Systems of the Onboard Avionics Aerospace and Transport Equipment of New Generation".

E-mail: lysenko\_av@bk.ru

ORCID iD: <https://orcid.org/0000-0002-7324-0190>



**Igor Kochegarov** graduated from Penza State University in 2000. In 1999, he started to work at the university – at first as a Laboratory Assistant, then as an Assistant Lecturer and Senior Lecturer. He defended his research thesis in 2005. At the moment he is the Deputy Head of the Department for Research. Research interests are IT in design of RS, mathematical modeling, development of micro-controller devices. He is the author of more than 150 publications, among which 15 are in top-rated peer-reviewed research journals. He is the author of 4 university textbooks. He has 2 patents of invention, 4 computer programme certificates.

E-mail: kipra@mail.ru

ORCID iD: <https://orcid.org/0000-0002-6821-5353>



**Vladimir Roganov**, Ph.D. (1997), Associate Professor (2000). He graduated from Novocherkassk Polytechnic Institute in 1978, undertook postgraduate studies at Riga Polytechnic Institute in 1983. He is the author of more than 120 scientific papers.

He worked as an Engineer at the Specialized Design Bureau (1978–1979) (Novorossiysk), as an Assistant at Shakhtinsky Technological Institute (1979–1981, 1984–1986) (Shakhty), Head of the Era Aircraft Simulator Association (1986–1995) (Penza), Director of the Center for Informatization of the Culture System of the Penza Region (1995–1998) (Penza), Associate Professor, Professor of Penza State University (1998–2012) (Penza), Director General of Video3 LLC (since 2008) (Penza), Professor of Penza State Technological University and (since 2012), Professor of Penza State University of Architecture and Construction (since 2017). He is a laureate

---

of the All-Russian Exhibition Center, academician of the International Academy of Education Informatization, serial entrepreneur.  
E-mail: [Vladimir\\_roganov@mail.ru](mailto:Vladimir_roganov@mail.ru)  
ORCID iD: <https://orcid.org/0000-0002-4498-9821>



**Jurijs Lavendels** Professor, *Dr. sc. ing.* His current research interests include computation methods with discretization and algebraization for design and modelling physical processes.  
E-mail: [Jurijs.Lavendels@rtu.lv](mailto:Jurijs.Lavendels@rtu.lv)  
ORCID iD: <https://orcid.org/0000-0002-8448-4705>